THE ASTROPHYSICAL JOURNAL, 307:L65–L68, 1986 August 15

EXTENDED FAR-INFRARED EMISSION ASSOCIATED WITH MASS OUTFLOWS FROM YOUNG STARS: L1551 IRS 5

S. EDWARDS,[1] S. E. STROM,[2] R. L. SNELL,[2] T. H. JARRETT,[2] C. A. BEICHMAN,[3] AND K. M. STROM[2]
Received 1986 March 19; accepted 1986 May 9

ABSTRACT

IRAS coadded survey data of a 1° × 1° field centered on the dark cloud L1551 reveals extended 60 and 100 μm emission aligned with the axis of the collimated molecular outflow from IRS 5. The correspondance of the far-infrared emission with the high-velocity molecular gas, while not exact, suggests strongly that the infrared emission is associated with the outflow from IRS 5. The luminosity of the extended infrared emission is considerable, equalling 18% of the bolometric luminosity of IRS 5 itself, and exceeding the mechanical luminosity in the expanding molecular gas by more than an order of magnitude. The distribution of the infrared surface brightness and the 60/100 μm color temperature is used to evaluate several possible mechanisms which might give rise to the observed emission.

Subject headings: interstellar: matter — nebulae: individual — stars: pre–main-sequence — stars: winds

I. INTRODUCTION

The early evolution of all young stars probably includes at least one episode of energetic, collimated mass loss. The observational evidence for these energetic outflows comes from phenomena associated with the dynamical interaction of supersonically expanding gas with surrounding interstellar matter. Wind mechanical luminosities determined from the swept-up, outflowing molecular gas range between 0.2% and 2% of the source radiative luminosity. The resultant dynamical pressure on the interstellar surroundings is probably sufficient to support molecular clouds against gravitational collapse (see Lada 1985).

The mechanical luminosities inferred from the expanding molecular gas, although considerable, may not reveal the true magnitude of the energy in the wind. Luminosities implied by mass-loss rates and velocities believed to characterize the stellar winds can be an order of magnitude greater than those seen in the expanding molecular gas. Radiative losses from the wind/cloud interaction zone could account for the discrepancy between the original and the observed wind luminosities. Using *IRAS* co-added survey data, we have begun to search young stellar object (YSO) mass outflow regions and have found a number of cases where extended infrared emission corresponds morphologically with other tracers of outflows from young stars. Preliminary findings for L1551 IRS 5 and its archetypical collimated outflow have been reported by Strom and Strom (1985) and Strom *et al.* (1986). This region has also been investigated by Clark and Laureijis (1986) with the *IRAS* survey sky flux images, at a lower sensitivity and spatial resolution. Their work confirms our finding of extended infrared emission aligned with the axis of the bipolar molecular outflow from IRS 5. Our results for the L1551 region are presented here.

[1] Five College Astronomy Department, Smith College.
[2] Five College Astronomy Department, University of Massachusetts.
[3] IPAC, California Institute of Technology.

II. OBSERVATIONS

The L1551 dark cloud lies in a southern extension of the fragmented and filamentary complex in Taurus that is the site of low-mass star formation. The L1551 cloud is roughly circular in projection, with an angular diameter of nearly 1° (2.8 pc at a distance of 160 pc), and a mass of about 80 $M_\odot$ (Snell 1981). It nurtures several T Tauri stars and low-luminosity infrared sources, the most active of which is IRS 5, a 38 $L_\odot$ YSO powering an energetic, bipolar wind that is collimated on scales from several arcsec to 30′ (Snell, Loren, and Plambeck 1980; Strom, Strom, and Vrba 1976; Emerson *et al.* 1984; Snell *et al.* 1985). The wealth of observational data for this bipolar outflow, which includes collimated blueshifted and redshifted lobes of supersonically expanding molecular gas, high-velocity HH objects, and optical and radio continuum jets, is summarized in recent articles by Strom *et al.* (1986) and Snell *et al.* (1985).

The *IRAS* survey data were coadded for 24 individual passes through the L1551 region to give a 1° × 1° field centered on IRS 5. This co-added format (*IPAC User's Guide* 1985) provides increased sensitivity and spatial resolution over the standard data product sky flux maps. The background subtraction procedure established at IPAC has been followed, in which a uniformly sloping plane is determined from the field edges. The procedure is satisfactory as long as no bright sources lie near the periphery of the field. This is verified by inspection of the SKYFLUX HCON-3 images. Table 1 lists the pixel sizes, the angular resolution (empirically determined from point sources in the co-added field), and the median noise after background subtraction for each of the four *IRAS* bands in the L1551 co-added field. Source intensities will be described in signal-to-noise units of the median noise given in Table 1.

Our data are presented in Figures 1 and 2 (Plates L6–L9). Figure 1 shows digital images for each of the four *IRAS* bands in the co-added L1551 field. In Figure 2*a*, the 60 μm

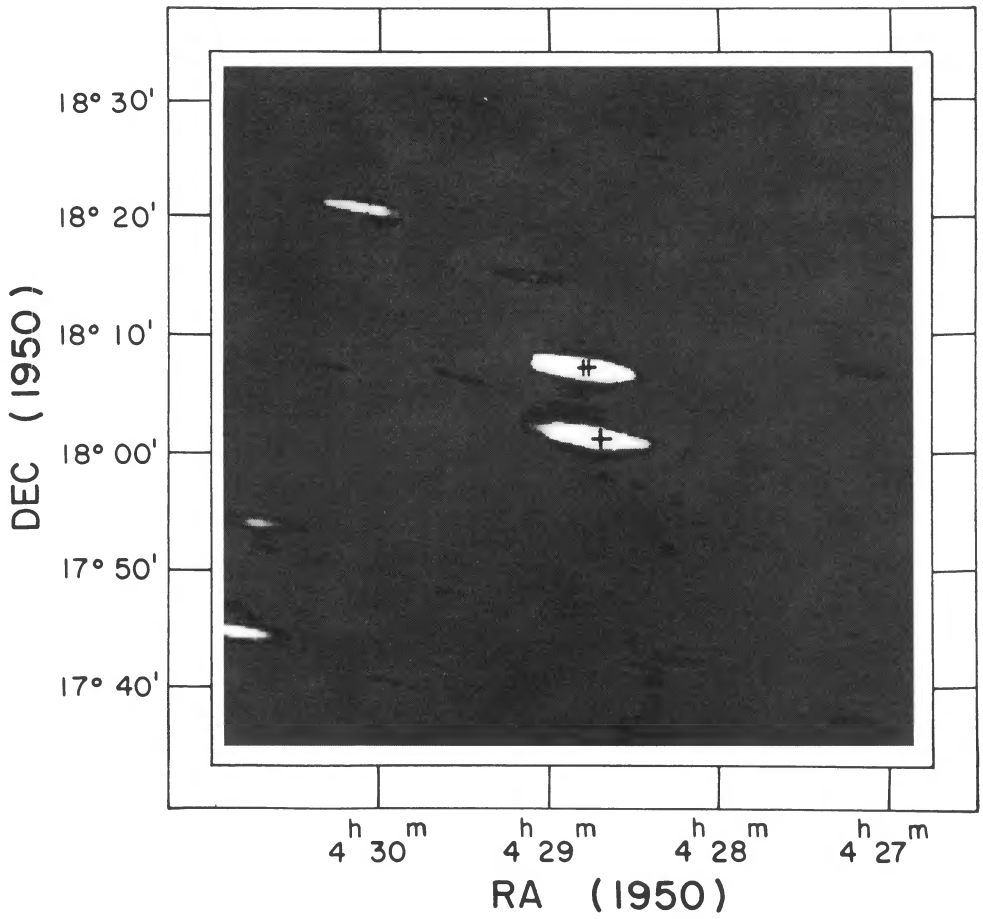

FIG. 1*a*

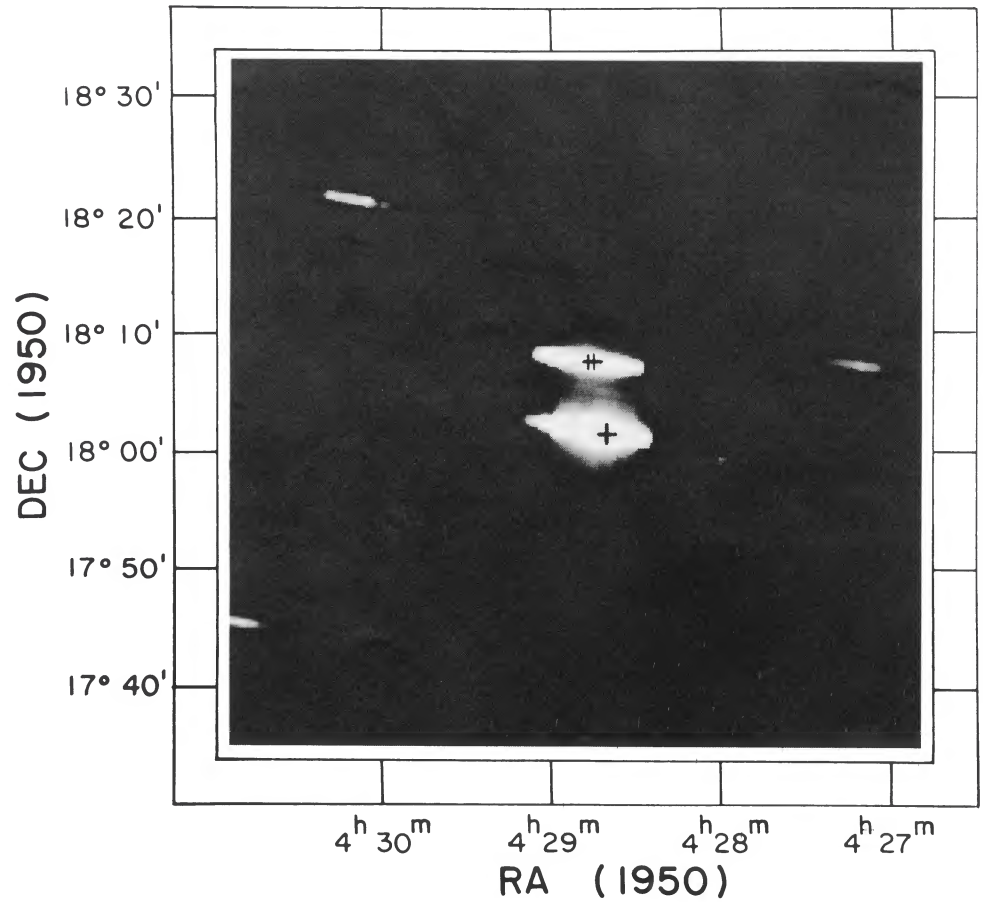

FIG. 1.—Images of the L1551 coadded field are shown for each of the four *IRAS* bands. IRS 5 and HL/XZ Tau are located by plus signs and HH 28 by a filled triangle. (*a*) and (*b*): The 12 and 25 μm images are linearly stretched between 2 σ (*black*) and 100 σ (*white*) (see Table 1). The gray background corresponds to intensities less than 2 σ. (*c*) and (*d*): The 60 and 100 μm images are linearly stretched between 2 σ (*black*) to 20 σ (*white*) (see Table 1). The gray background corresponds to intensities less than 2 σ; intensities in excess of 20 σ are shown by contours in units of the median noise level. For the 60 μm image, the contours correspond to 24, 48, 190, 540, and 1530 σ; for the 100 μm image, the contours correspond to 24, 36, 100, 200, and 830 σ.

EDWARDS *et al.* (*see* page L65)

FIG. 1*b*

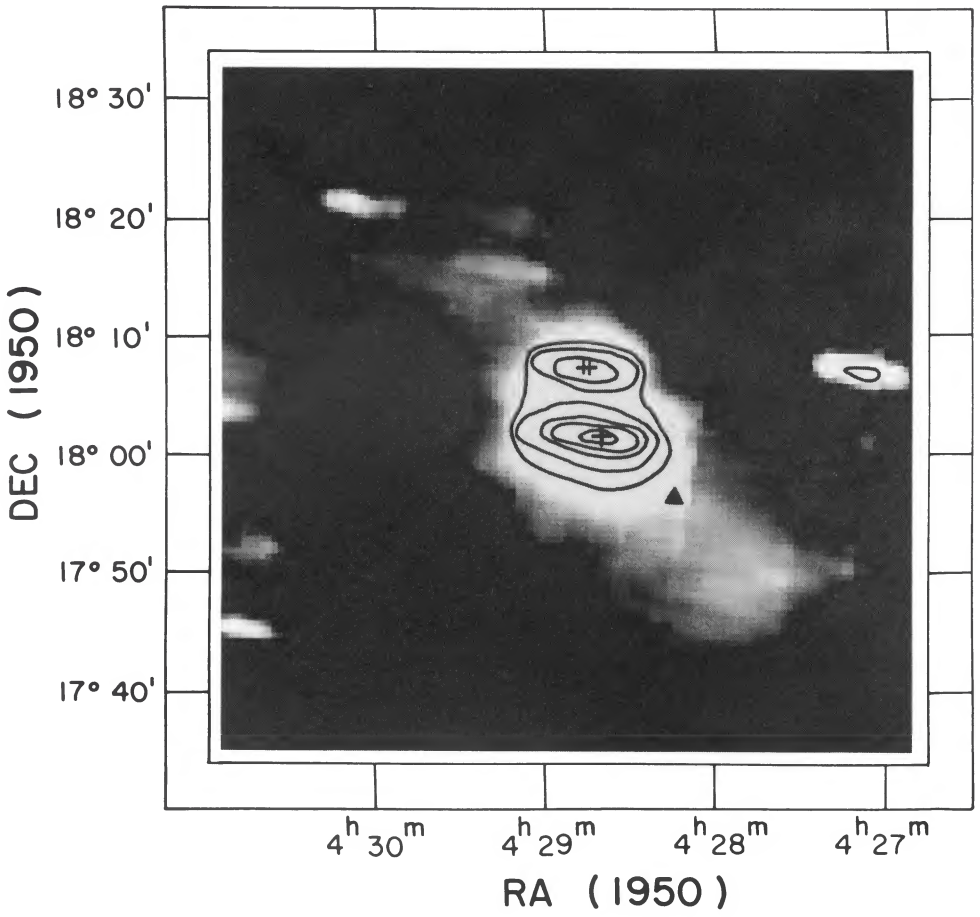

FIG. 1*c*

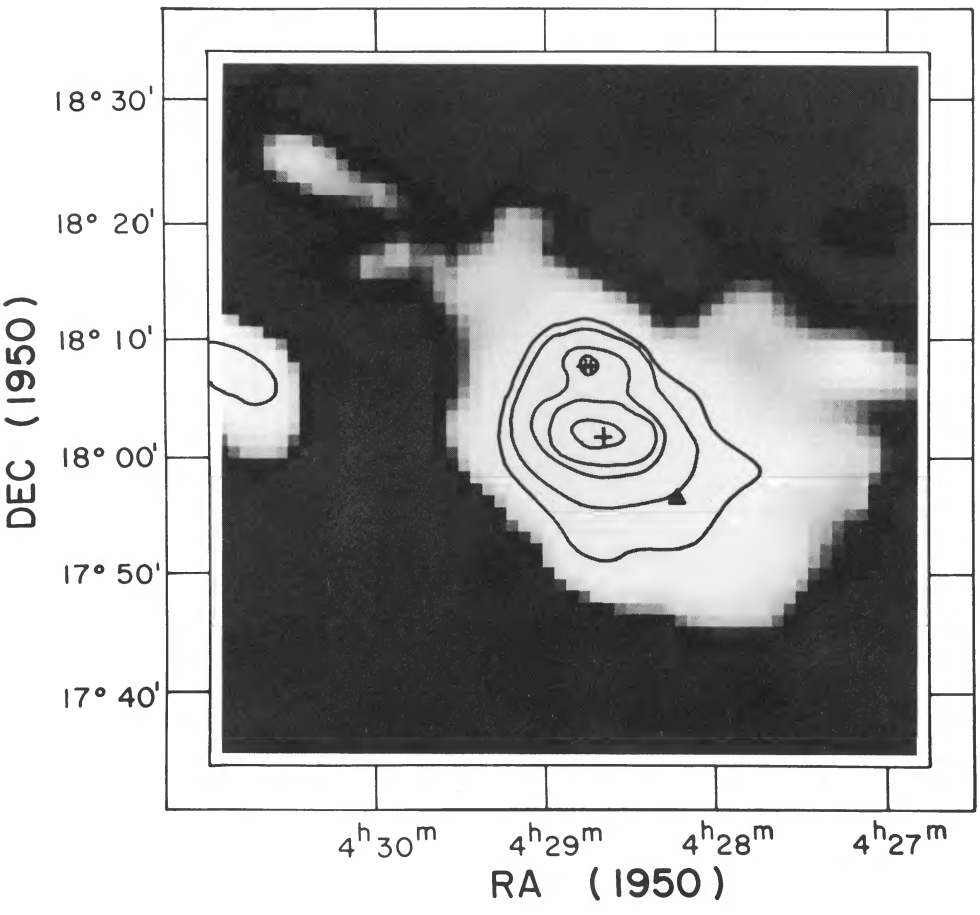

FIG. 1*d*

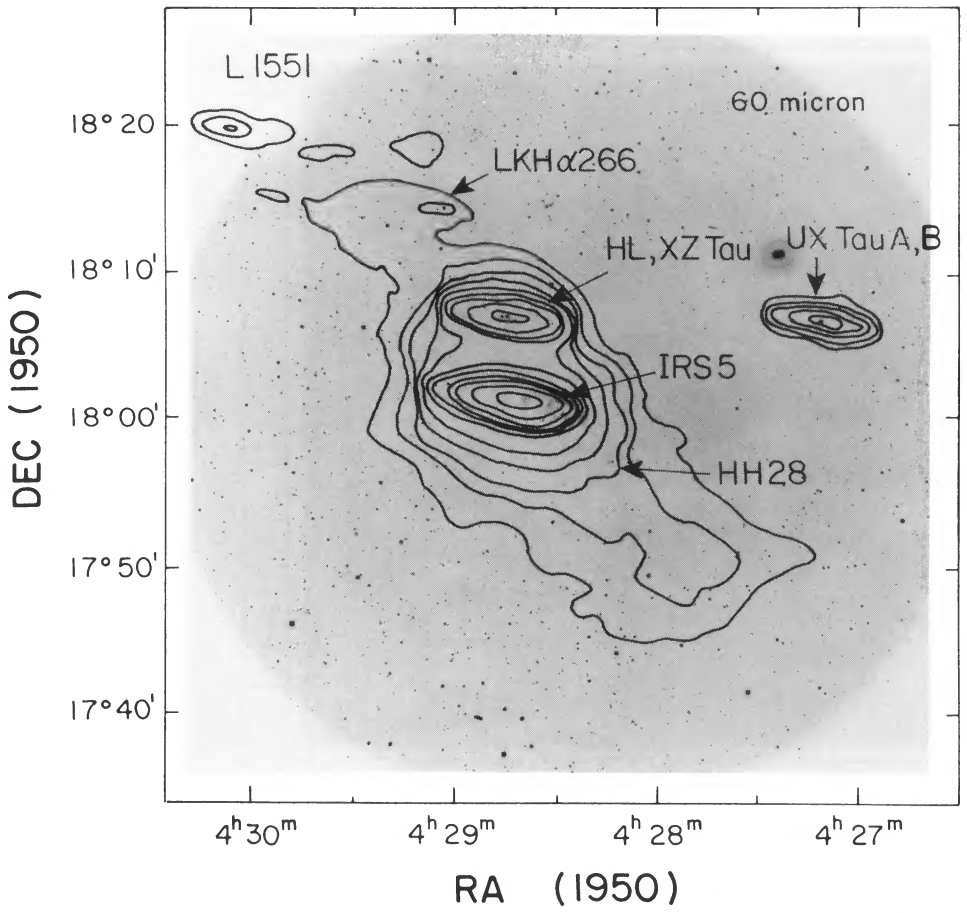

FIG. 2a

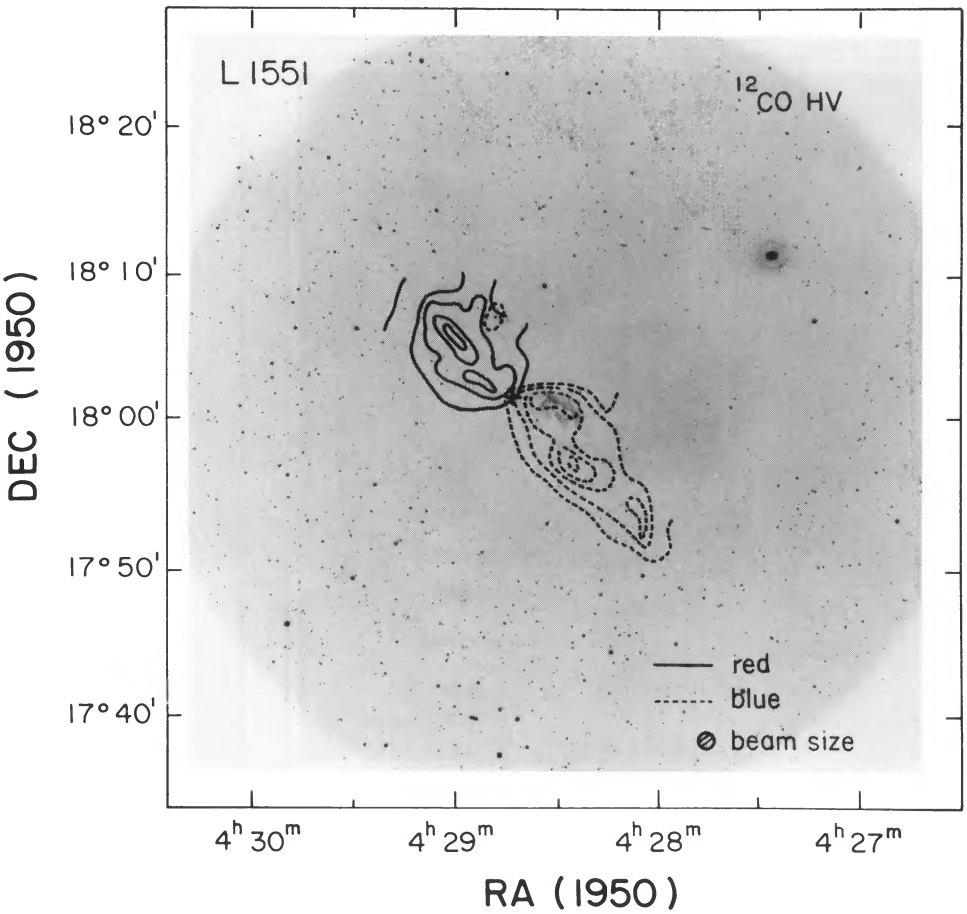

FIG. 2b

FIG. 2.—A broad-band *R* plate of the L1551 region, obtained with the prime focus camera of the Mayall 4 m telescope at KPNO, provides the background for the following contour maps: (*a*) The *IRAS* 60 μm intensity map from coadded survey data is contoured in units of the median noise level (Table 1); contours correspond to 4, 8, 12, 20, 34, 96, 192, 384, 768, 1535, and 3070 σ. (*b*) The integrated intensity of the high-velocity blueshifted (*dashed*) and redshifted (*solid*) molecular gas is contoured at intervals of 5 K km s^{-1}, with the lowest contour at a level of 5 K km s^{-1} (from Snell and Schloerb 1985). (*c*) The extent of the L1551 molecular cloud is shown in this map of the integrated intensity of the full ^{12}CO $J = 1–0$ line, with contour intervals of 2 K km s^{-1} beginning at a level of 2 K km s^{-1} (Snell 1981). The location of the young stellar objects IRS 5, HL/XZ Tau, UX Tau A, B and LkHα 266 plus HH 28 are labelled in Fig. 2*a*.

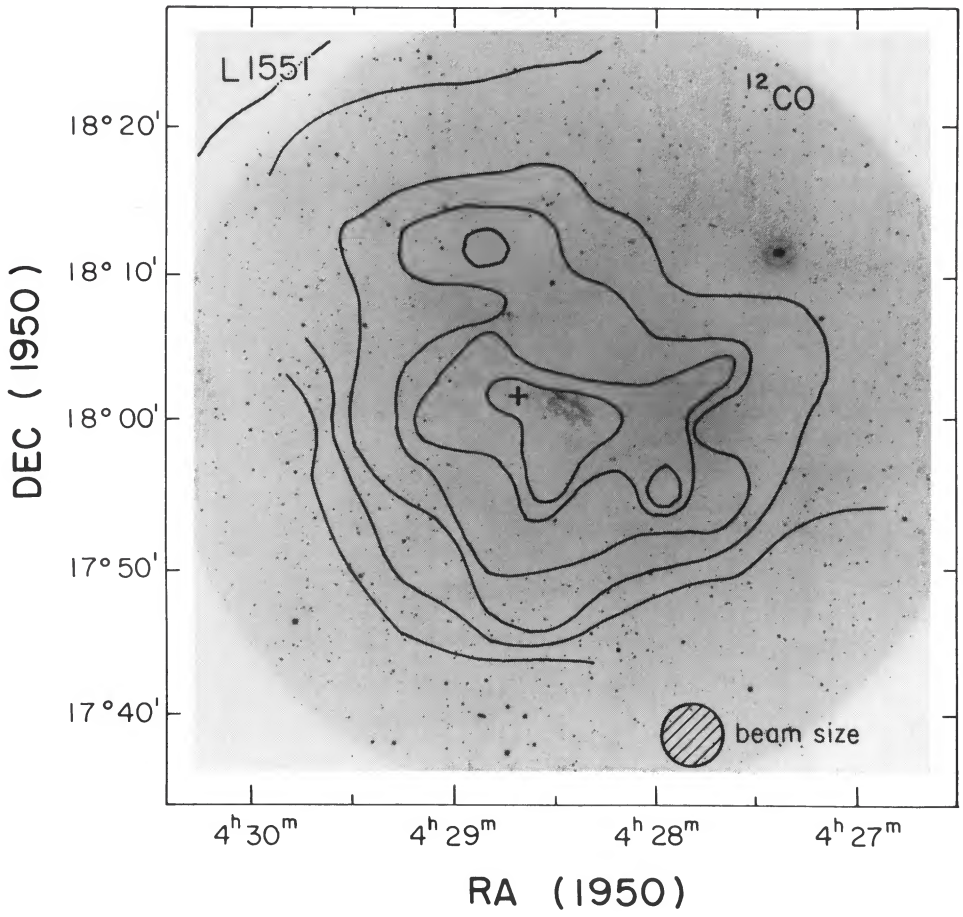

FIG. 2c

TABLE 1

L1551 *IRAS* DATA

Band	Pixel Size	Beam FWHP	Median Noise (Jy sr^{-1})
1.....	0.′25 × 0.′25	1′ × 3′	1.3×10^5
2.....	0.′25 × 0.′25	1′ × 3′	2.1×10^5
3.....	0.′5 × 0.′5	1.′5 × 4′	1.1×10^5
4.....	1 × 1	3′ × 5′	3.4×10^5

contours are superposed over a broad-band *R* plate of the L1551 region, taken with the 4 m Mayall telescope at KPNO. For comparison, in Figures 2*b* and 2*c*, contours of the ^{12}CO high-velocity gas (Snell and Schloerb 1985) and the overall ^{12}CO emission delineating the L1551 cloud (Snell 1981) are overlaid on the same *R* plate. The location of several YSOs are indicated in Figures 1 and 2; additional *IRAS* sources which may be YSOs are also seen; they will be discussed at a later time.

From the data presented in Figures 1 and 2 we note the following:

1. Extended 60 and 100 μm emission is aligned along the outflow axis defined by the collimated supersonic molecular gas. Although no extended emission is seen at 12 or 25 μm, at 60 and 100 μm extended emission is seen to the southwest and the northeast of IRS 5. The extended infrared emission bears little morphological similarity to the spherical L1551 cloud (Fig. 1*c*) but instead is closely aligned with the axis of the molecular outflow from IRS 5 (Fig. 1*b*). As with the molecular emission, in the infrared, the southwest (blueshifted) lobe is more extended and more luminous than the northeast (redshifted) lobe.

2. The morphological correspondance between the outflowing molecular gas and the collimated infrared emission is not exact. In order to facilitate a direct comparison of the molecular and infrared emission, we have convolved the ^{12}CO high-velocity molecular data with the *IRAS* 60 μm beam. This is shown in Figure 3 (Plate L10), where the contours of the convolved high-velocity molecular emission are overlaid on the 60 μm co-added image.

To the southwest of IRS 5, the 60 μm emission is more extended than the outermost (2 K km s^{-1}) contour of integrated high velocity molecular emission. This is shown in Figure 4, where the 60 μm surface brightness is plotted against radial distance along the outflow axis, 8′–22′ from IRS 5. The surface brightness is nearly constant over this interval, extending an additional 5′ (0.2 pc) beyond the outermost contour of the high velocity gas, which terminates 15′ (0.7 pc) from IRS 5. Perpendicular to the outflow axis, a low surface brightness "halo" of 60 μm emission (2–4 σ) extends 4′–8′ beyond the 2 K km s^{-1} boundary of the high-velocity molecular gas.

To the northeast of IRS 5, the 60 μm emission includes several stellar sources, including HL/XZ Tau and LkHα 266, preventing any firm conclusion about the correspondance between the infrared emission and the redshifted molecular gas in this region. At 100 μm, the degraded resolution leads to considerable source confusion, both in the southwest and in the northeast, although the general elongation of 100 μm emission along the molecular outflow axis is still apparent.

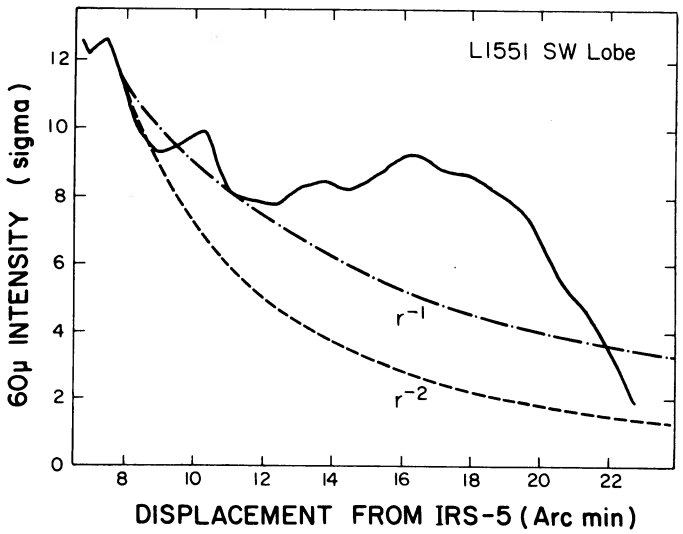

FIG. 4.—The 60 μm surface brightness is plotted as a function of distance from IRS 5, measured along the southwest outflow axis (0.1 pc = 2′).

III. RESULTS

a) The Luminosity of the Extended Infrared Emission

The integrated 60 and 100 μm luminosity of the extended infrared emission enclosing IRS 5 is 3 $L_\odot$. This includes all emission $\geq 2\ \sigma$ around IRS 5 but excludes the contribution of the YSOs IRS 5, HL/XZ Tau, UX Tau A, B, and LkHα 266. (The 60 + 100 μm luminosities of these YSOs are 10 $L_\odot$, 2 $L_\odot$, 0.1 $L_\odot$, and 0.02 $L_\odot$, respectively.) Extrapolation based on a color temperature of 24 K (see below) yields a bolometric luminosity of 7 $L_\odot$ for the extended infrared emission.

This exceeds the mechanical luminosity in the high-velocity molecular gas ($L_{HV} = 0.2\ L_\odot$; Snell and Schloerb 1985) by over an order of magnitude. The infrared luminosity is comparable, however, to the mechanical luminosity implied by the mass outflow rate and velocity, $10^{-6}\ M_\odot$ yr^{-1} and 300 km s^{-1}, respectively, inferred for IRS 5 (Snell and Schloerb 1985; Strom *et al.* 1986). If the radiative luminosity does derive from the IRS 5 outflow, then the wind luminosity is 18% of the stellar luminosity, rather than 1% as determined from the expanding molecular gas.

b) The Color Temperature and Dust Mass of the Extended Infrared Emission

In Figure 5 (Plate L11) we present a map of the 60/100 μm color temperature for the L1551 co-added field. The 60 μm data have been degraded to the resolution of the 100 μm map, a (wavelength)$^{-1}$ emissivity law has been assumed, and the 60/100 μm flux density ratio has been subjected to the appropriate calibrations and color corrections as described in Beichman *et al.* (1984) and the *IPAC Users Guide* (1985). Data with an intensity below 2 σ at 100 μm or 1.5 σ at 60 μm have been eliminated in this figure.

Several temperature components are apparent in the southwest lobe of extended emission. An inner "core" region of fairly uniform color temperature (24–25 K) lies along the

PLATE L10

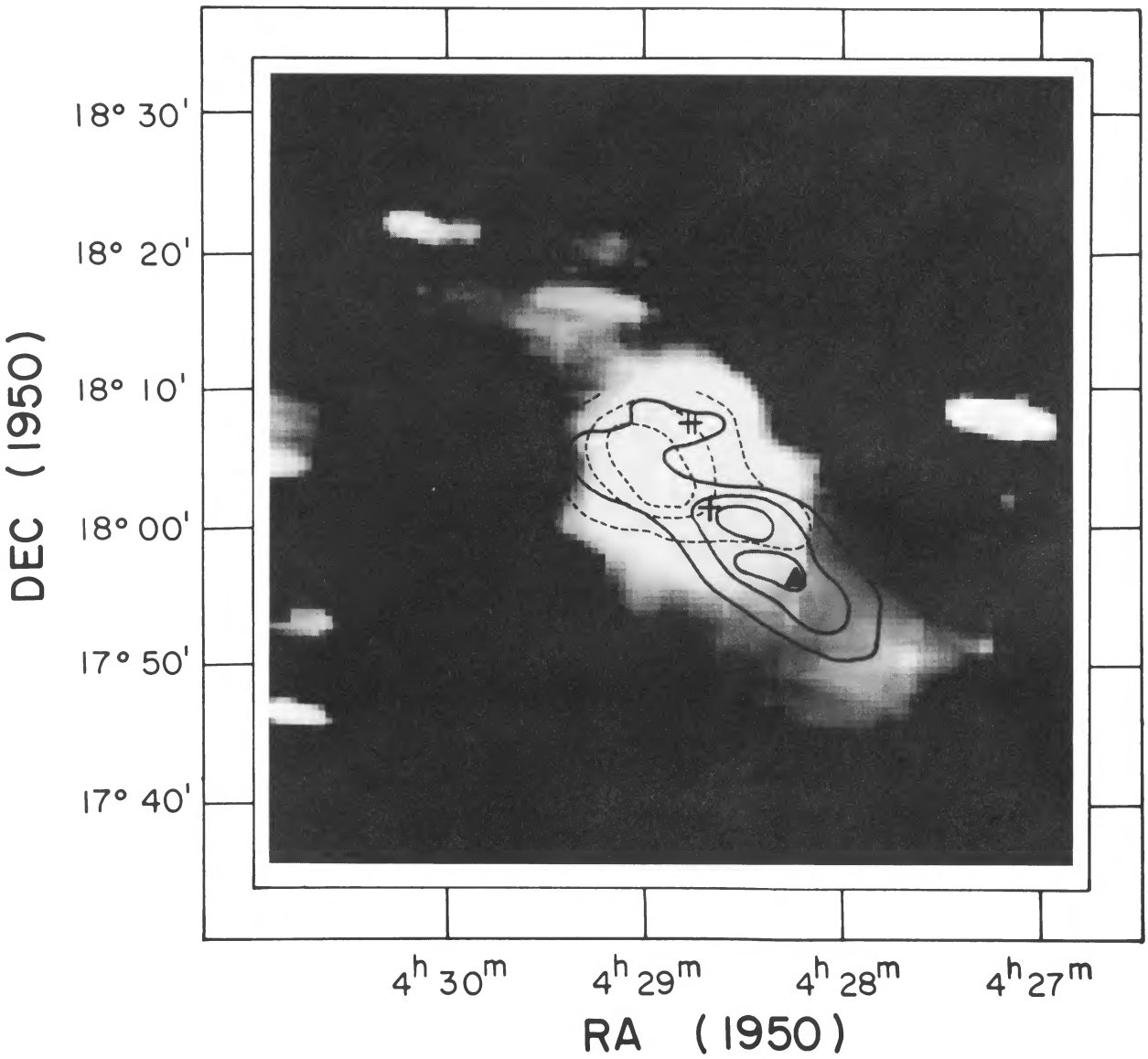

FIG. 3.—The map of the high-velocity molecular emission from Fig. 2*b* has been convolved with the *IRAS* 60 μm beam and contoured at levels of 2, 8, and 14 K km s^{-1}. The molecular contours are overlaid on the 60 μm image from Fig. 1*c*. The plus signs mark the position of IRS 5, HL Tau, and XZ Tau; the filled triangle locates HH 28.

EDWARDS *et al.* (*see* page L66)

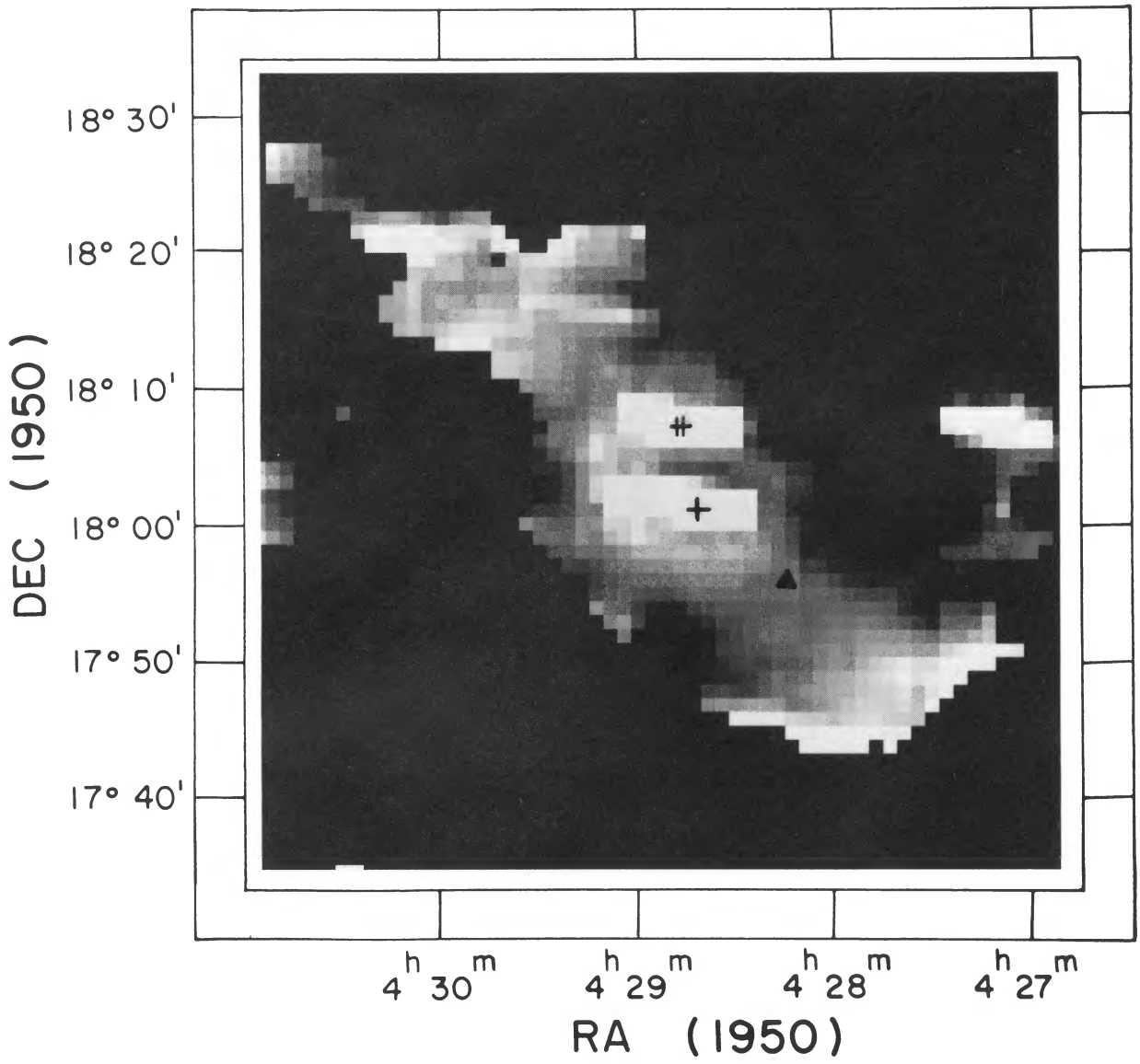

FIG. 5.—The 60/100 μm color temperature map of the L1551 coadded field. The image is linearly stretched between 20 K (*black*) and 35 K (*white*). The gray background includes some positions where no color temperature is determined (i.e., with 60 and/or 100 μm intensities below 1.5 or 2.0 σ, respectively; see Fig. 1). The positions of IRS 5, HL Tau, and XZ Tau are shown by plus signs and HH 28 is shown by a filled triangle.

EDWARDS *et al.* (*see* page L66)

outflow axis, with a width perpendicular to the axis which is comparable to that of the high-velocity molecular gas. This "core" is surrounded by a broader, cooler (20∃123 K) "halo" extending 4′–8′ beyond the confines of the high-velocity molecular gas. A third, but somewhat uncertain, component is an apparent temperature rise to about 30 K on the extreme periphery of the southwest lobe, coincident with the edge of the L1551 cloud. It is possible that this apparent temperature rise on the edge of the extended emission is a result of a systematic baseline error in the co-added utility.

If the extended far infrared emission is thermal emission from dust grains, the dust mass required to explain the observed emission is about 0.02 $M_\odot$. This estimate follows from the observed 60 μm surface brightness, the derived color temperature, and the assumptions of a (wavelength)$^{-1}$ emissivity law and normal interstellar grain properties. The dust optical depths were calculated for each pixel position and have values on the order of 10^{-4} to 10^{-5}. If a normal gas/dust ratio of 100 is assumed, the corresponding gas mass of 2 $M_\odot$ is comparable to the 1 $M_\odot$ estimated to comprise the expanding molecular material (Snell and Schloerb 1985).

IV. DISCUSSION

The alignment of the extended far-infrared emission with the axis of the IRS 5 outflow argues strongly that it is physically associated with IRS 5 and its wind. Radiative heating from IRS 5 cannot be a major source of dust excitation. The equilibrium temperature at a distance of 1 pc from IRS 5 expected from a normal mix of interstellar grains is only 12 K. An appropriate mix of small grains, transiently heated by stellar photons, could produce an elevated and uniform color temperature via time-averaged fluctuations in thermal emission (see Sellgren 1984). However, a decrease in surface brightness with distance from IRS 5, proportional to r^{-2}, should then result, in sharp contrast to the behavior shown in Figure 4.

We therefore conclude that the IR emission derives from the mechanical energy in the IRS 5 wind. Both thermal emission from dust grains and line emission from atomic or molecular species in shock cooling regions (Genzel and Stacey 1985) could be important radiators at 60 and 100 μm. At this time, we briefly examine some implications of dust grain emission; a more detailed look at emission mechanisms will be included in a later paper.

If the infrared emission is from dust grains heated through dissipation of the mechanical energy of the wind from IRS 5, this could occur either via (1) collisional heating at the wind-cloud interface or (2) radiative heating from the shock cooling region at the wind-cloud interface. Collisional heating of grains requires densities on the order of 10^4 cm^{-3} for gas/dust coupling to occur at the kinetic temperatures of 24–25 K, as shown by Clark and Laureijis (1986). Such densities would necessarily be confined to the immediate vicinity of the molecular outflow, where significant compression of the cloud material has occurred.

The observed extension of the infrared emission beyond the boundary of the expanding molecular gas necessitates an alternate means of transferring the wind energy to the surrounding dust. A stellar wind of several 100 km s^{-1} impacting a molecular shell expanding at tens of km s^{-1} might produce a spectral energy distribution from the shock cooling region similar in character to HH objects. As an example, in HH 1 the line plus continuum ultraviolet luminosity (1200–3000 Å) exceeds the optical luminosity (3200–11000 Å) by a factor of 20 (Böhm, Böhm-Vitense, and Brugel 1981). The penetration depth of such shock-cooling photons can be estimated as follows. The extinction from the flow boundary to the cloud boundary may be estimated from the ^{13}CO column density (Snell 1981) to be $A_v \approx 1$ and $A_{1500\,\text{Å}} \approx 3.7$, assuming a (wavelength)$^{-1}$ opacity law. The UV photons would penetrate the cloud a few arc minutes (a few tenths of a parsec) from the molecular shell, as seen. The rapid decline in 60 μm surface brightness about 5′ from the wind/cloud interface shown in Figure 4 would result from a rapid decrease in optical depth, as this region coincides with the edge of the L1551 cloud outlined by the ^{12}CO in Figure 1*c*.

In this scenario, a marginally detectable level of optical photons might escape the cloud. For example, if 1/20 of the observed far-infrared emission originates as optical photons, equally distributed between 3000 and 11000 Å and uniformly distributed over the flow area, an A_v of 1 yields a surface brightness at $V = 25$ mag arcsec^{-2}. If some fraction of the IR emission originates from collisionally heated dust or IR shock-cooling lines, then the optical surface brightness would be correspondingly lower.

V. CONCLUSIONS

Co-added *IRAS* survey data have been examined in the L1551 region. The major results of this study are the following:

1. Extended low surface brightness 60 and 100 μm emission is aligned with the molecular outflow from L1551 IRS 5. The morphology and the uniform surface brightness and color temperature of the IR emission suggest that the wind from IRS 5 is the source of this emission.

2. The luminosity of the extended infrared emission is considerable, with $L_{IR}/L_{HV} = 35$ and $L_{IR}/L_\odot = 0.18$. At this time, we favor radiative heating of grains by photons generated at the stellar wind/cloud interface as a major contributor to the extended infrared emission.

Conclusions regarding the ubiquity and cause of this phenomenon await our analysis of additional outflow regions. If a characteristic set of spatial and spectral properties of extended infrared emission can be identified from the outflows under study, it is possible that the *IRAS* data base may be used to locate YSOs currently undergoing massive outflows and thereby provide a means of assessing the true frequency of this important phase in pre–main-sequence evolution.

We would like to thank the staff at IPAC, especially W. Rice and J. Good, for help and assistance above and beyond their duties as *IRAS* "friends"; and the staff of the Digital Image Analysis Lab at the University of Massachusetts, including D. M. Chesley, D. Oliver, and R. Newton. We are grateful for the timely appearance of the Five College Astronomy Image Analysis Laboratory, supervised by S. Kleinmann. This work was supported by NASA/JPL contract 957271.

REFERENCES

Beichman, C. A., Neugebauer, G., Habing, H. J., Clegg, P. E., and Chester, T. J. 1984, *IRAS Explanatory Supplement.*
Böhm, K. H., Böhm-Vitense, E., and Brugel, E. W. 1981, *Ap. J. (Letters)*, **245**, L113.
Clark, F. O., and Laureijs, R. J. 1986, *Astr. Ap.*, **154**, L26.
Emerson, J. P., Harris, S., Jennings, R. E., Beichman, C.A., Baud, B., Beintema, D. H., Marsden, P. L., and Wesselius, P. R. 1984, *Ap. J. (Letters)*, **278**, L49.
Genzel, R., and Stacey, G. J. 1985, *Mitt. Astr. Ges.*, No. 63, p. 215.
Lada, C. 1985, *Ann. Rev. Astr. Ap.*, **23**, 267.
Sellgren, K. 1984, *Ap. J.*, **277**, 623.
Snell, R. L. 1981 *Ap. J. Suppl.* **45**, 121.
Snell, R. L., Bally, J., Strom, S. E., and Strom, K. M. 1985, *Ap. J.*, **290**, 587.
Snell, R. L., Loren, B., and Plambeck, R. L. 1980, *Ap. J. (Letters)*, **239**, L17.
Snell, R. L., and Schloerb, P. 1985, *Ap. J.* **295**, 490.
Strom, S. E., and Strom, K. M. 1985, in *IAU Symposium 115, Star Forming Regions,* in press.
Strom, S. E., Snell, R. L., Jarrett, T., Edwards, S., Strom, K. M., and Beichman, C.A. 1986, *Bull. AAS*, **17**, 837.
Strom, S. E., Strom, K. M., and Vrba, F. 1976, *A. J.*, **81**, 320.

C. A. BEICHMAN: IPAC, Mail Stop 100-22, California Institute of Technology, Pasadena, CA 91125

S. EDWARDS: Five College Astronomy Department, Smith College, Northampton, MA 01063

T. H. JARRETT, R. L. SNELL, K. M. STROM, and S. E. STROM: Five College Astronomy Department, University of Massachusetts, Amherst, MA 01003

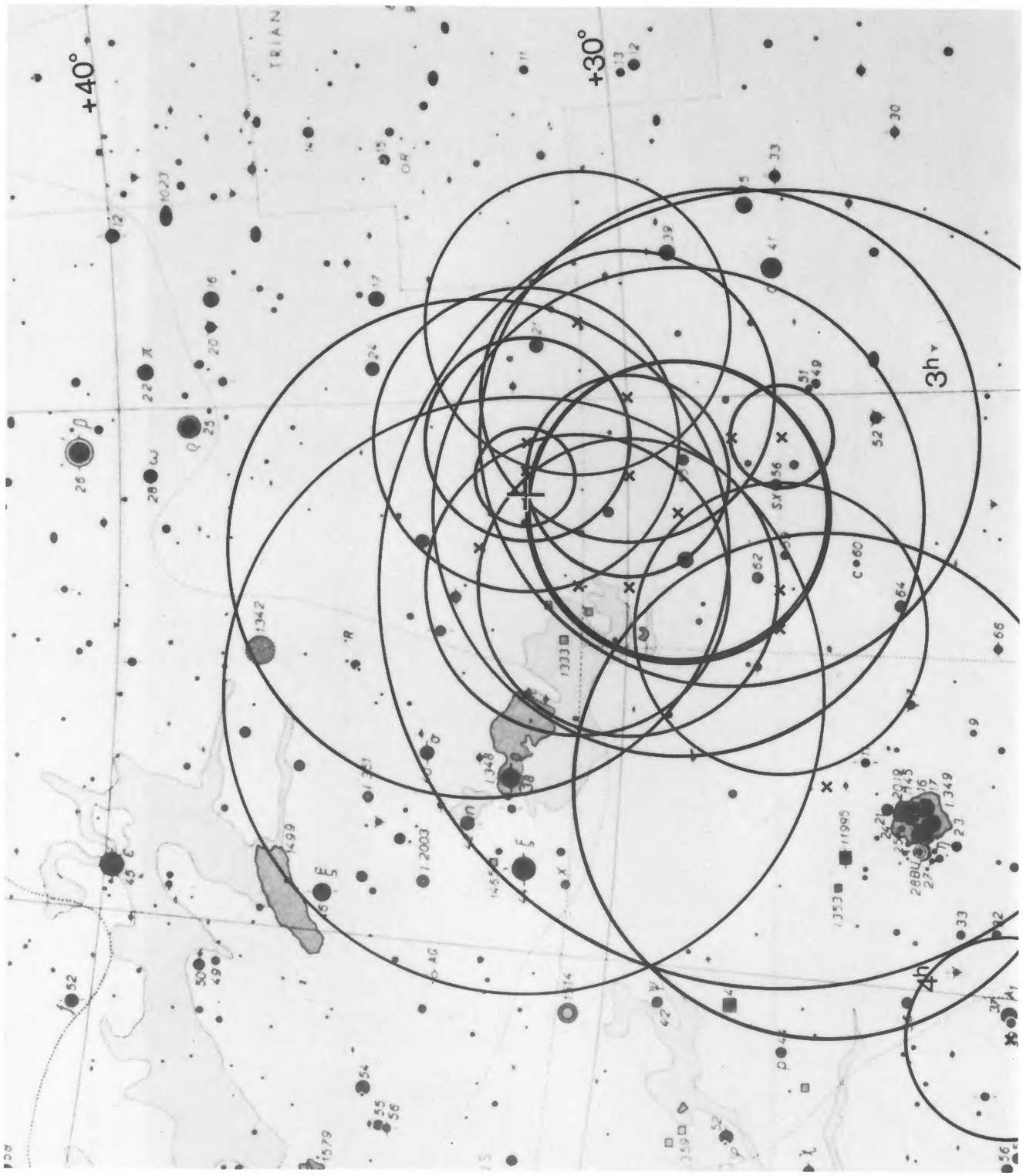

FIG. 3*a*.—Wide-field chart. This section from the Skalnate Pleso *Atlas of the Heavens* (epoch 1950.0) covers roughly the central third of the survey area. The photographic flash position is marked with a large "plus." Each visual sighting (Table 1) is indicated by a cross and error circle. Note that the circles 48+29+3 and 48+29+5 each represent three observations. Most of the flashes appear clustered in a small region of the survey area.

KATZ *et al.* (*see* page L35)

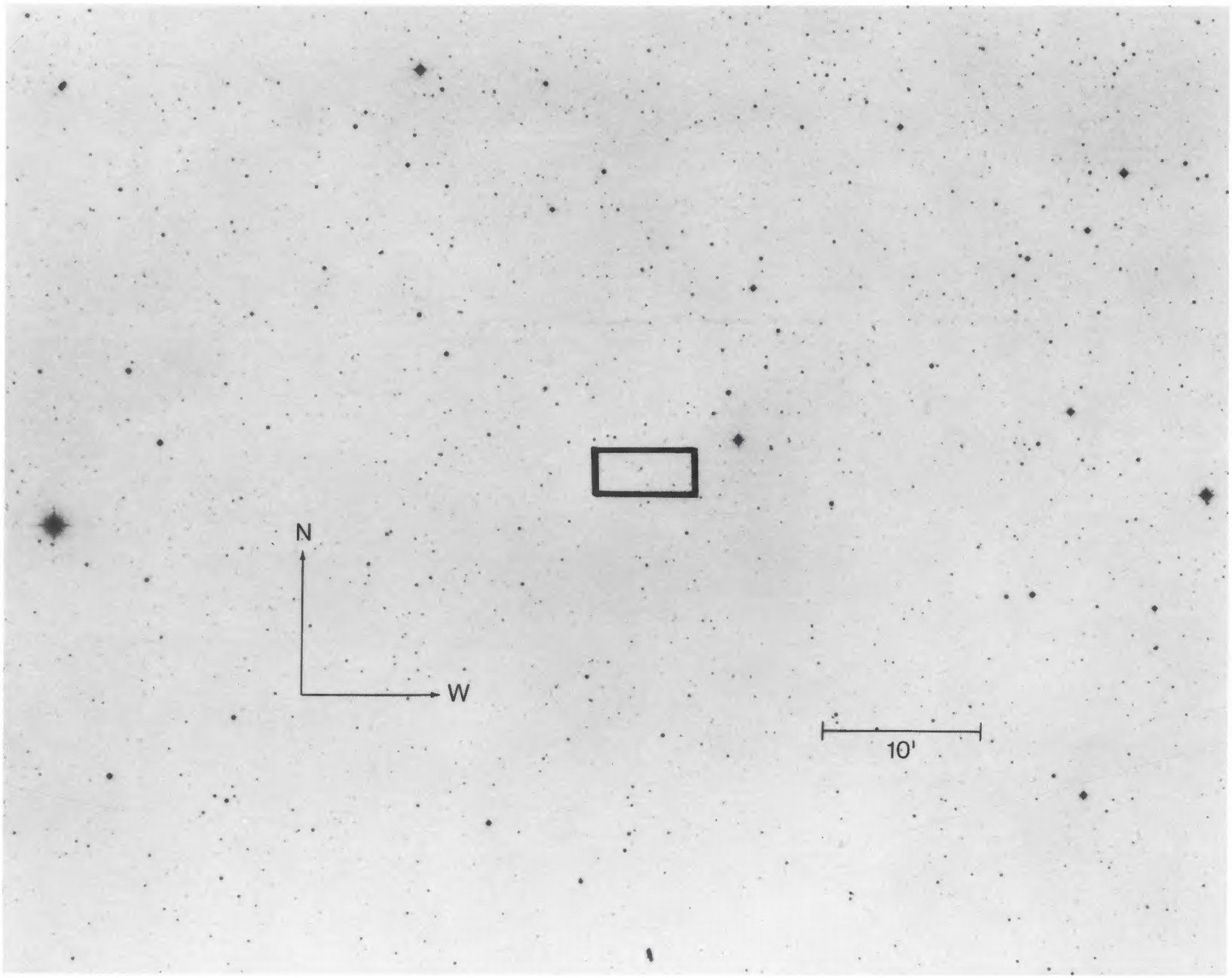

FIG. 3*b*.—Narrow-field chart. The field displayed has been reproduced from the POSS O plate copy of the David Dunlap Observatory (Copyright © by the National Geographic Society-Palomar Observatory Sky Survey. Reproduced by permission from the California Institute of Technology). The error box associated with the photographic flash position is marked. The brightest star in the box has a photographic magnitude of about 17 in the blue and 16 in the red (King and Raff 1977).

KATZ *et al.* (*see* page L36)